Concatemerization of tRNA molecules in the presence of trivaline derivative

Sergey A. Streltsov*, Larissa P. Martinkina, Yuri Yu. Vengerov

Engelhardt Institute of Molecular Biology, Russian Academy of Sciences, Vavilov str. 32, Moscow 117984, Russia

Received 19 October 1998; received in revised form 10 December 1998

Abstract The interaction of tRNA with trivaline dansyl hydrazide trifluoroacetate (DHTV) has been studied. The shape of curves of fluorimetric titration of tRNA with DHTV and vice versa can be explained only by formation of DHTV dimers on tRNA molecules, and subsequent association of DHTV-saturated tRNA molecules with each other. The ability of tRNA molecules to form concatemers in solution in the presence of DHTV has been demonstrated by electron microscopy. Electron microscopy of the tRNA-DHTV complexes stained with uranyl acetate revealed flexible rods 6–7 nm thick and up to several micrometers long.

Key words: Concatemer; Nucleic acid-peptide interaction; tRNA; Trivaline

1. Introduction

In early 1970s, several models were proposed for recognition of double-stranded regions in nucleic acids by proteins with β-structures [1–3]. Such proteins were really found [4–7]. In some of these cases the β-structure was localized in the DNA minor groove [8–10]. On the other hand, the model proposed by Gursky et al. [3] stimulated the investigation of nucleic acid binding with short peptides able to acquire a β-structure. Trivaline (DHTV) [11], longer linear peptides [12–15], as well as peptides joined by SS bridges (for additional stabilization of β-structure) were synthesized [16–18]. All peptides were adsorbed in the DNA minor groove and were specific towards different nucleotide sequences. The DHTV dimer binding on nucleic acids was highly cooperative [19,20]. DHTV formed monomeric and β-dimeric complexes on single-stranded polymers [21], and, in addition to these types, β-sandwich peptide structures [19] were observed on double-stranded polymers. Profound similarity was found between DHTV binding to single- and double-stranded polymers. This made possible the improvement of the above-mentioned model [22] and the development of a universal model explaining the formation of the following nucleopeptide structures: (1) a pseudoduplex structure made by two single-stranded nucleic acid molecules positioned side by side and saturated with DHTV forming β-dimers [21]; (2) quadruplex structures consisting of two nucleic acid duplexes or pseudoduplexes with DHTV bound in the form of β-sandwiches [21,22]. Such quadruplex structures could result from peptide-peptide or nucleo-nucleic interaction [22]; they were both later confirmed in experiments [23]. The quadruplex structures could give rise to 'higher order compact' structures [21,22] containing several quadruplex units arranged side by side and concatemeric structures in which numerous quadruplex units could be aligned one after another. In the presence of DHTV, such structures were formed by some trinucleotides [24] in such a way that addition of condensing agents caused covalent binding of the trinucleotides into chains containing up to 12 nucleotides [25]. In this work, tRNA concatemerization in the presence of DHTV was demonstrated by electron microscopy. The concatemers had the appearance of flexible rod structures 6–7 nm thick, and reaching several micrometers in length. Basing on the fluorescence intensity measurements, it can be supposed that the concatemer flexible rod structures are formed by tRNA molecules after their saturation with the peptide in dimeric form and further association of tRNA-bound peptide dimers giving rise to quadruplex nucleopeptide structures.

2. Materials and methods

2.1. Reagents

DHTV was synthesized as described in [19]. Sodium cacodylate (Sigma, USA), *Escherichia coli* $tRNA_{\Sigma}$ (BDH, UK), and freshly distilled MeOH were used in this work. The DHTV-tRNA complexes were prepared as described in [23].

2.2. Spectral measurements

Optical densities of DHTV and tRNA solutions were determined in a Cary-118C spectrophotometer (Varian, USA). The molar extinction coefficients were taken to be $\varepsilon_{330} = 3800\ M^{-1}\ cm^{-1}$ for DHTV in MeOH and $\varepsilon_{260} = 7500\ M^{-1}\ cm^{-1}$ (average per phosphate) for $tRNA_{\Sigma}$ in buffer. The concentration of tRNA is given in mol tRNA phosphates. Fluorescence intensity was measured in a MPF-2A spectrofluorimeter (Hitachi, Japan). A high sensitivity cell attachment and a 4 mm optical path cell were used. The fluorescence was excited and registered at 400 and 500 nm, respectively, with a 20 nm slit for both. Changes in gain during the experiments were corrected using a fluorescence standard. Fluorescence intensity is given in arbitrary units. All measurements were done in 1 mM cacodylate buffer, pH 6.7 in the presence of 25% MeOH.

2.3. Electron microscopic experiments

Specimens were prepared as described in [26], and examined in a JEM-100CX electron microscope (JEOL, Japan) at an accelerating voltage of 80 kV and screen magnification 5000–20 000×. Contour lengths were measured with a digitizer-equipped computer.

3. Results and discussion

3.1. Formation of the DHTV dimeric complex on tRNA

We have titrated tRNA solutions with DHTV to find out whether DHTV molecules interact with tRNA. Fig. 1 shows the results of fluorimetric titration of 2.16×10^{-5} M $tRNA_{\Sigma}$

*Corresponding author. Fax: (7) (095) 1351405.
E-mail: strelcov@imb.imb.ac.ru

Abbreviations: DHTV, trivaline dansyl hydrazide trifluoroacetate

PII: S0014-5793(99)00072-1

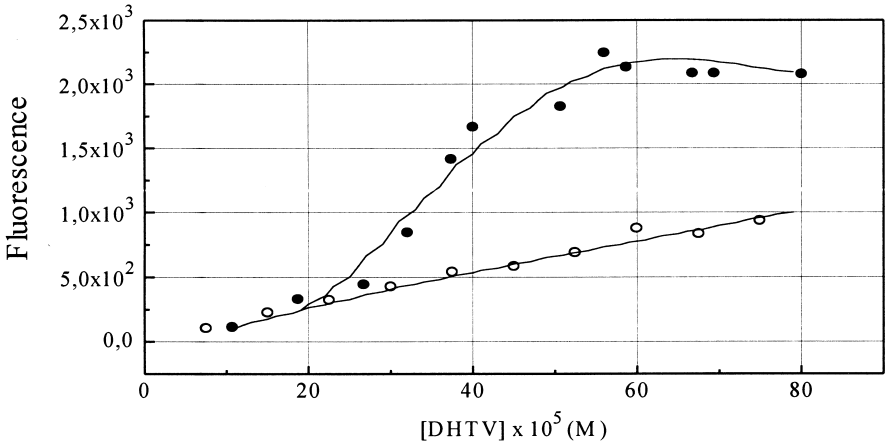

Fig. 1. Dependence of DHTV fluorescence intensity on its concentration in the absence (curve 2) and in the presence of 2.16×10^{-5} M tRNA (curve 1). $\lambda_{ex}=400$ nm, $\lambda_{em}=500$ nm. Fluorescence intensity is given in arbitrary units. Buffer: 1 mM sodium cacodylate, pH 6.7 and 25% (vol.) MeOH, 20°C.

(curve 1) and buffer (curve 2) with DHTV. Both curves coincide at low DHTV concentrations. Then, a non-linear increase in peptide fluorescence intensity is observed as the DHTV concentration becomes higher. It is of interest to compare the experimental curve with the theoretical dependence, which can be calculated assuming that for each type of complex the fluorescence intensity is linearly dependent on peptide concentration. The concentrations of tRNA-bound peptide monomers and dimers will be designated y_1 and y_2, respectively. According to the law of mass action, they depend on the tRNA and free peptide concentrations P and C, respectively, as $y_1=K_1\ (P-n_1{\cdot}y_1)C$ and $y_2=K_2\ (P-n_2{\cdot}y_2)C^2$, where K_1 and K_2 are constants of DHTV monomer and dimer binding with tRNA, n_1 and n_2 give the number of tRNA bases occupied, respectively, by DHTV monomer and dimer upon binding. Then, division of the variables will give

$$y_1 = K_1{\cdot}P{\cdot}C/(1+K_1{\cdot}n_1{\cdot}C)\quad y_2 = K_2{\cdot}P{\cdot}C_2/(1+K_2{\cdot}n_2{\cdot}C_2) \qquad (1)$$

Both equations are valid if the DHTV concentrations used are much higher than the tRNA concentrations, which really was the case. The slope of these curves, $d(y_1 1)/dC$ and $d(y_2)/dC$, respectively, will depend on the peptide concentration as $d(y_1)/dC=K_1{\cdot}P/(1+K_1{\cdot}n_1{\cdot}C)^2$ and $d(y_2)/dC=2K_2{\cdot}P{\cdot}C/(1+K_2{\cdot}n_2{\cdot}C^2)^2$

Thus, the slope of the theoretical curve describing the peptide monomer binding decreases as the DHTV concentration in solution is increased, which does not agree with the experimental data. However, in the case of the peptide dimer binding, the slope of the theoretical curve increases with the peptide concentration. Thus, the shape of experimental curves demonstrates formation on tRNA of at least a dimeric complex of the peptide.

3.2. Interaction of DHTV-saturated tRNA molecules with each other

We have titrated DHTV solution with tRNA to find out whether the DHTV-saturated tRNA molecules interact with each other. DHTV was taken in a concentration (3.7×10^{-4} M) at which mostly peptide dimers are adsorbed on tRNA molecules (Fig. 1). The results of fluorimetric titration are shown in Fig. 2. Fig. 2a shows the whole curve, while Fig. 2b demonstrates its beginning. A non-linear increase in the peptide fluorescence intensity is observed as the tRNA concentration becomes higher. To check whether interaction of tRNA molecules saturated with peptide takes place, it is of interest to analyze the theoretical dependences admitting and excluding such interactions, and to compare the experimental curve (Fig. 2b) with the theoretical dependences. The curve presented in Fig. 2b corresponds to $C>P$ and Eq. 1 is valid. Since the cooperativity of the DHTV dimer binding to nucleic acid is very high [19,20], in the presence of DHTV in solution there are either free or peptide-saturated tRNA molecules. In this case the ratio $y_3=y_2/n_3$ is valid, where y_3 is the concentration of peptide-saturated tRNA molecules, n_3 is the mean number of DHTV molecules adsorbed on a single tRNA molecule. If it is assumed that the peptide-saturated tRNA molecules do not interact with each other, then after differentiation of Eq. 1 with respect to P, replacing y_2 in it with y_3, we obtain $d(y_3)/dP=K_2{\cdot}C^2/(n_3\ (1+K_2{\cdot}n_2{\cdot}C^2))$, i.e. the slope of the curve decreases as the tRNA concentration becomes higher. Such a curve does not coincide with the experimental one shown in Fig. 2b. However, on the assumption that two peptide-saturated tRNA molecules interact with each other with the constant K_4, different results are obtained. According to the law of mass action, $y_4=K_4\ (y_3-2y_4)^2$, where y_4 is the concentration of the associates formed. If we consider the initial region of this dependence, then $y_3>y_4$ and $y_4=K_4{\cdot}(y_3)^2/(1+4K_4{\cdot}y_3)$. Substitute y_3 in Eq. 1. Then, $y_3=P\ \ (K_2{\cdot}C^2/(n_3\ \ (1+K_2{\cdot}n_2{\cdot}C^2)))$. Denote $B=K_2{\cdot}C^2/(n_3\ (1+K_2{\cdot}n_2{\cdot}C^2))$. Then, $y_4=K_4{\cdot}B^2{\cdot}P^2/(1+4K_4{\cdot}B{\cdot}P)$, and $d(y_4)/dP=P{\cdot}B^2{\cdot}K_4$ $(1/(1+4K_4{\cdot}B{\cdot}P)+1/(1+4K_4{\cdot}B{\cdot}P)^2)$. This equation describes a curve whose slope becomes higher as the tRNA concentration is increased. Thus, the shape of the curve shown in Fig. 2b can be explained assuming interaction between two or more peptide-saturated tRNA molecules. The results of this theoretical analysis are valid at any ratio of fluorescence intensity of individual tRNA-DHTV complexes and their associates.

3.3. Electron microscopic studies of concatemerization of DHTV complexes with tRNA

The complexes obtained were then studied by electron microscopy. Only in cases when intermolecular associates of tRNA molecules saturated with DHTV were formed according to fluorescence experiments, flexible rod structures were observed in electron microscopic preparations. Microphoto-

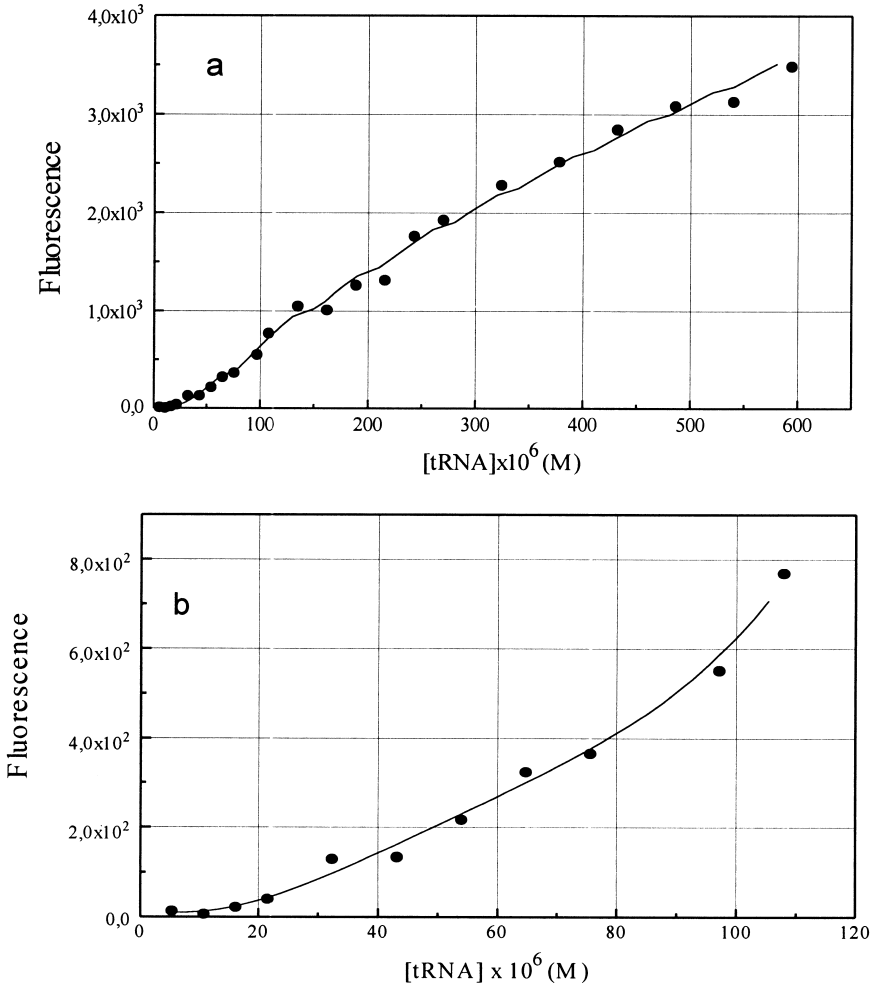

Fig. 2. Dependence of the DHTV fluorescence intensity on tRNA concentration. a: The whole curve. b: The region of low tRNA concentrations. Concentration of DHTV 3.7×10^{-4} M. The fluorescence intensity of free DHTV was subtracted. Other conditions as in Fig. 1.

graphs of these particles stained with uranyl acetate are shown in Fig. 3 (the concentration of DHTV was 3.7×10^{-4} M and that of $tRNA_{\Sigma}$ 2.16×10^{-5} M). The structures observed were homogeneous in thickness (6–7 nm) and heterogeneous in length, which significantly exceeded that of the original tRNA molecules. The average number of bases in a tRNA molecule is 83 ± 10, and the average distance between the bases is 0.32 nm. Then, the length of completely stretched tRNA molecules is 27 ± 4 nm. The lengths of the concatemer structures were measured. The results for 82 structures are

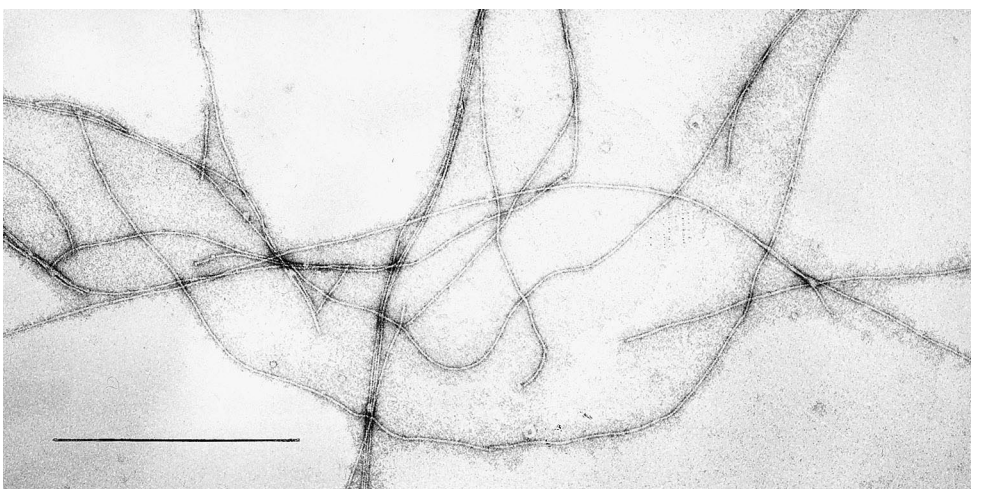

Fig. 3. Microphotographs of DHTV complex with tRNA. Concentration of $tRNA_{\Sigma}$ 2.16×10^{-5} M; concentration of DHTV 3.7×10^{-4} M. Preparations were stained with 2% aqueous uranyl acetate. Bar corresponds to 500 nm.

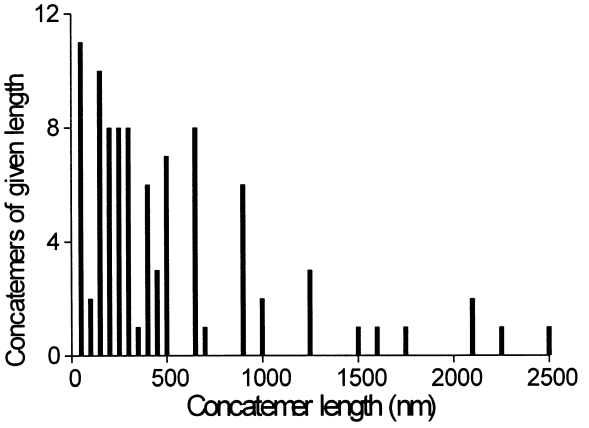

Fig. 4. Histogram of lengths of concatemer structures. In total, 82 structures were measured. Bar height corresponds to the number of structures of given length.

summarized in the histogram in Fig. 4. It is seen that the flexible rod structures formed in the presence of DHTV may be several dozen times longer than the original tRNA molecules. In our opinion, this is due to concatemerization of intermolecular (quadruplex) complexes of DHTV with tRNA molecules. In control experiment without DHTV, no concatemer structures of tRNA were detected by electron microscopy.

4. Conclusion

Concatemerization of nucleic acids has been studied for many years [27–29]. The model of double-stranded polymer concatemerization via 'sticky ends' was proposed in 1972 [30]. It is also applicable to the description of concatemerization of some single-stranded oligonucleotides [29]. However, we are dealing with concatemerization of nucleopeptide complexes, probably quadruplex structures. Thus some trinucleotides with DHTV formed flexible rod structures over 100 nm in length [24]. It is possible that polyU concatemerization in the presence of DHTV took place in [20], but polyU are linear. In contrast, tRNA molecules have a complex spatial organization, with a secondary cloverleaf structure [31] folded in a tertiary one [32]. However, even such molecules are able to form concatemers in solution in the presence of DHTV.

Acknowledgements: The authors are indebted to the colleagues from the Engelhardt Institute of Molecular Biology Drs. O.F. Borisova and A.N. Surovaya for the courtesy of *E. coli* $tRNA_{\Sigma}$, Dr. N.B. Ul'yanov for help in obtaining dansyl preparations, and G.V. Serdyukov for technical assistance in electron microscopy. The work was partly supported by the Russian Foundation for Basic Research (Grants 94-04-49047 and 96-04-49186) and the State Program for Support of Russian Scientific Schools (96-105-98093).

References

[1] Carter, Ch.W. and Kraut, J. (1974) Proc. Natl. Acad. Sci. USA 71, 75–90.
[2] Kim, S.-H., Sussman, J.L. and Church, G.M. (1975) in: Structure and Conformation of Nucleic Acids and Protein-Nucleic Acids Interactions (Sundaralingam, M. and Rao, T.S., Eds.), pp. 571–575, University Park Press, Baltimore, MD.
[3] Gursky, G.V., Tumanyan, V.G., Zasedatelev, A.S., Zhuze, A.L., Grokhovsky, S.L. and Gottikh, B.P. (1975) Mol. Biol. (Russ.) 5, 635–651.
[4] Allain, F.H.-T., Howe, P.W., Neuhaus, D. and Varani, G. (1997) EMBO J. 16, 5764–5774.
[5] Valegard, K., Murray, J.B., Stonehouse, N.J., van der Worm, S., Stockley, P.G. and Lilias, L. (1997) J. Mol. Biol. 270, 724–738.
[6] Raumann, B.E., Rould, M.A., Pabo, C.O. and Sauer, R.T. (1994) Nature 367, 754–757.
[7] Kim, X., Geiger, J.H., Hahn, S. and Singler, P.B. (1993) Nature 365, 512–520.
[8] Rice, P.A., Yang, S.-W., Mizuuchi, K. and Nash, H.A. (1996) Cell 87, 1295–1306.
[9] Clark, K.L., Halay, E.D., Lai, E. and Burley, S.K. (1993) Nature 364, 412–420.
[10] White, S.W., Appelt, K., Wilson, K.S. and Tanaka, L. (1989) Proteins 5, 281–288.
[11] Streltsov, S.A., Khorlin, A.A., Surovaya, A.N., Gursky, G.V., Zastdatelev, A.S., Zhuze, A.L. and Gottikh, B.P. (1980) Biofizika (Russ.) 25, 929–940.
[12] Surovaya, A.N., Streltsov, S.A., Khorlin, A.A., Gursky, G.V., Nechipurenko, Yu.D., Zhuze, A.L. and Gottikh, B.P. (1982) Stud. Biophys. 87, 189–190.
[13] Gursky, G.V., Zasedatelev, A.S., Zhuze, A.L., Khorlin, A.A., Grokhovsky, S.L., Streltsov, S.A., Nikitin, S.M., Mikhailov, M.V., Surovaya, A.N., Rechinsky, V.O., Beabealashvilly, R.Sh., Krylov, A.S. and Gottikh, B.P. (1983) Cold Spring Harbor Symp. Quant. Biol. 47, 361–372.
[14] Sidorova, N.Yu., Semenov, T.E., Surovaya, A.N., Vengerov, Yu.Yu., Streltsov, S.A., Khorlin, A.A., Gottikh, B.P., Zhuze, A.L. and Gursky, G.V. (1987) Mol. Biol. (Russ.) 21, 1534–1550.
[15] Vengerov, Yu.Yu., Semenov, T.E., Surovaya, A.N., Sidorova, N.Yu., Streltsov, S.A., Khorlin, A.A., Zhuze, A.L. and Gursky, G.V. (1988) J. Biomol. Struct. Dynam. 6, 311–330.
[16] Grokhovsky, S.L., Surovaya, A.N., Sidorova, N.Y.u, Votavova, X., Sponar, Ya., Frich, I. and Gursky, G.V. (1988) Mol. Biol. (Russ.) 22, 1315–1333.
[17] Grokhovsky, S.L., Surovaya, A.N., Brussov, R.V., Chernov, B.K., Sidorova, N.Yu. and Gursky, G.V. (1991) J. Biomol. Struct. Dynam. 8, 989–1025.
[18] Grokhovsky, S.L., Surovaya, A.N., Zhuze, A.L. and Gursky, G.V. (1994) Mol. Biol. (Russ.) 28, 1137–1148.
[19] Makarov, V.L., Streltsov, S.A., Vengerov, Yu.Yu., Khorlin, A.A. and Gursky, G.V. (1983) Mol. Biol. (Russ.) 17, 1089–1101.
[20] Streltsov, S.A., Lysov, Yu.P., Semenov, T.E., Vengerov, Yu.Yu., Khorlin, A.A., Surovaya, A.N. and Gursky, G.V. (1991) Mol. Biol. (Russ.) 25, 1040–1060.
[21] Streltsov, S.A., Semenov, T.E. and Moroz, O.V. (1993) Mol. Biol. (Russ.) 27, 1183–1198.
[22] Streltsov, S.A., Semenov, T.E. and Moroz, O.V. (1993) Mol. Biol. (Russ.) 27, 1165–1182.
[23] Streltsov, S.A., Borodina, M.V. and Semenov, T.E. (1996) J. Biomol. Struct. Dynam. 14, 357–363.
[24] Streltsov, S.A., Martinkina, L.P., Khorlin, A.A., Florentiev, V.L., Vengerov, Yu.Yu., Zhenodarova, S.M., Sedelnikova, E.A. and Smolyaninova, O.A. (1994) J. Biomol. Struct. Dynam. 11, 1403–1415.
[25] Streltsov, S.A., Khorlin, A.A., Victorova, L.S., Kochetkova, S.V., Tsilevich, T.L. and Florentiev, V.L. (1992) FEBS Lett. 298, 57–60.
[26] Martinkina, L.P., Kolesnikov, A.A., Streltsov, S.A., Yurchenko, V.Yu. and Vengerov, Yu.Yu. (1998) J. Biomol. Struct. Dynam. 15, 949–957.
[27] Carlson, K. (1968) J. Virol. 2, 1230–1237.
[28] Quadrifoglio, F., Manzini, D., Dikelspiel, K. and Crea, R. (1982) Nucleic Acids Res. 10, 3759–3768.
[29] Yolov, A.A., Gromova, E.S., Romanova, E.A., Dretskaya, T.S., Oganova, A.A., Buryanov, Ya.I. and Shenodarova, Z.A. (1984) FEBS Lett. 167, 147–150.
[30] Watson, J.D. (1972) Nature New Biol. 239, 197–201.
[31] Holley, R.W., Apgar, J., Everett, G.A., Madison, J.T., Marquisee, M., Merrill, S.H., Penswick, J.R. and Zamir, A. (1965) Science 147, 1462–1465.
[32] Kim, S.-H., Suddath, F.L., Quigley, G.J., McPherson, A., Sussman, A., Wang, A.H.J., Seeman, N.C. and Rich, A. (1974) Science 185, 436–440.